Coupling of Marine Circulation and Wind-Wave Models on Parallel Platforms

Dr. David Welsh and Dr. Keith Bedford
Dept. of Civil and Environmental Engineering and Engineering Graphics
The Ohio State University

Rong Wang and Dr. Ponnuswamy Sadayappan
Dept. of Computer and Information Science
The Ohio State University

Abstract

Accurate predictions of wave heights, currents, and water elevations are vital in the planning of military operations in the marine environment. Marine circulation and wind-wave models have traditionally been run separately, but recent research has identified potentially important interactions between current and wave motions. The aim of this paper was to couple advanced circulation and wave models to take full advantage of the CEWES MSRC high performance computing facilities. Results are presented from the coupling of the MPI parallel CH3D code and the OpenMP parallel WAM code using the SGI ORIGIN 2000 platform. Communication between the models is achieved using MPI. Lake Michigan hindcasts show that wave-current inter actions have a significant effect on storm surges and the associated currents. Scalability results are given for the individual codes and the coupled system. The effect of grid size on scalability is also investigated.

Introduction

Accurate predictions of wave heights, currents, and water elevations are vital in the planning of military operations such as amphibious landings, fleet navigation, and search and rescue missions. Marine circulation and wind-waves have traditionally been modeled independently. It has recently been suggested, however, that there can be significant interactions between the two motions at both the atmospheric boundary layer (Holthuijsen and Tolman, 1991) and the marine bottom boundary layer (Glenn and Grant, 1987). Work has been done on coupled models in the last decade, but simplified models have generally been used due to the performance limitations of sequential computer systems. The aim of this research was to couple advanced circulation and wave models to take full advantage of the CEWES MSRC high performance computing facilities. The coupling of parallel models has been completed at the atmospheric boundary layer and results are presented in this paper. In related research (Welsh et al., 1999), coupling is also underway at the bottom boundary layer.

Model Descriptions

The CH3D marine circulation model (Chapman et al., 1996) and WAM wind-wave model (WAMDI, 1988) were used in this research. Both codes contain advanced physics and their sequential versions have been used for several years at CEWES. CH3D predicts

the three-dimensional current, temperature, and salinity fields, and the two-dimensional water surface elevation field. The model solves conservation equations for mass, momentum, and thermal energy using finite difference discretizations on a curvilinear horizontal grid and a sigma layer (terrain following) vertical grid. A mode-splitting solution technique is used in which external (barotropic) and internal (baroclinic) motions are solved separately, allowing an enhanced baroclinic time-step. The external mode uses vertically-averaged equations to predict water surface elevations and mean horizontal velocities, then the internal mode re-introduces vertical variations. CH3D requires inputs of time-varying water surface winds and heat fluxes or air temperatures.

The WAM wind-wave model predicts frequency-direction spectra of wave energy on a regular grid; significant wave height, mean wave period, and mean wave direction are calculated from the spectra. WAM cycle 4 (Gunther et al., 1992) is used here. This version is based on the conservation of wave action density and includes advanced, "third-generation" physics (Komen et al., 1994) in the treatment of the wind input, nonlinear wave-wave interaction, and dissipation source terms. WAM includes algorithms for current-induced wave propagation and refraction, and for depth-induced refraction and shoaling. In the basic model, depth and current effects are assumed to be steady throughout a single simulation, but in this research unsteady current and depth effects were implemented (Zhang et al., 1998).

Parallel versions of CH3D and WAM have been developed as part of this research. One-dimensional domain decomposition was used in CH3D (Bangalore et al., 1999). A pre-processor divides the grid into a user-specified number of horizontal blocks. The blocks do not all contain the same number of rows. The number of water cells in a row will vary, so the number of rows in each block must be tailored to give approximately equal total numbers of water cells and, therefore, good load balancing. A two-dimensional decomposition was not selected since it would have made good load balancing difficult to attain. During the CH3D simulation the processors for neighboring blocks send each other updated arrays using MPI calls. A post-processor re-assembles each block's output files into grid-wide files, ready for visualization. A parallel version of WAM was obtained using the OpenMP library. The sequential code was first compiled with the Power Fortran Analyzer (PFA) argument to obtain suggestions for OpenMP directives. Beneficial directives were then identified by trial and error in the four most time-consuming subroutines, totaling 50 % of sequential model execution time. In the remaining subroutines all the PFA parallel directives were used.

Coupling Strategy and Physics

A coupled simulation involving MPI CH3D and OpenMP WAM is launched using the *mpirun* command, with one process specified for WAM and multiple processes specified for CH3D. The number of WAM threads to be used in parallel regions is set in the WAM shell script invoked in the *mpirun* command line. MPI is used for communication between the CH3D master process and WAM. Separate communicators are defined for intra-model communication within CH3D and inter-model communication.

The OpenMP library is only available at present for shared memory multi-processing architectures. All coupling operations in this research have, therefore, used the SGI ORIGIN 2000 (O2K) platform at CEWES MSRC. Cross-platform coupling will also be possible using the MPI_Connect library developed by the University of Tennessee at Knoxville. This library allows processes to communicate when they are running on different types of platforms at different locations. The operation of MPI_Connect was verified using harbor wave simulations running on three geographically distant O2K platforms (Bova et al., 1999).

Coupling physics at the atmospheric boundary layer requires the WAM model to send arrays of radiation stress and wave stress to CH3D. The radiation stress tensor, S_{ij}, results in the following surface momentum transfer components being added in CH3D's momentum conservation equation:

$$M_x = \frac{-1}{Hr_w}\left[\frac{\partial S_{xx}}{\partial x} + \frac{\partial S_{xy}}{\partial y}\right], \tag{1}$$

$$M_y = \frac{-1}{Hr_w}\left[\frac{\partial S_{xy}}{\partial x} + \frac{\partial S_{yy}}{\partial y}\right], \tag{2}$$

where H is water depth and r_w is water density. The radiation stress components are calculated in WAM using (Phillips, 1977)

$$S_{ij} = r_w g \int_0^{2p}\int_0^{\infty}\left[\frac{c_g}{c_p}\frac{k_i k_j}{k^2} + \left(\frac{c_g}{c_p} - \frac{1}{2}\right)d_{ij}\right]E(w,q)\,dw\,dq\,, \tag{3}$$

where g is gravitational acceleration, c_g is wave group speed, c_p is wave phase speed, k is wavenumber magnitude, k_i and k_j are wavenumber components, d_{ij} is the Dirac delta function, and $E(w,q)$ is the wave energy spectral density in frequency-direction space. Wave stress is the portion of wind stress caused by the presence of wind waves. This means that the wind stress calculated in WAM is used as the wave stress in CH3D. The presence of waves increases the surface roughness, leading to increased wind input into currents. This is accomplished in CH3D by using the wave stress in the calculation of the surface drag coefficient:

$$C_D = \left[k \,/\ln\left(\frac{L\sqrt{1-x}}{z_0}\right)\right]^2, \tag{4}$$

where k is the von Karman coefficient, = 0.4; L is a reference level for the wind velocity, = 10 m above mean water level; z_0 is the roughness height, which is iteratively

related to C_D; and x is the ratio of the wave stress to the total stress, with the total stress given by

$$t_t = r_a C_D |\tilde{u}_{10}| \tilde{u}_{10}, \tag{5}$$

where r_a is air density and $\tilde{u}_{10}$ is the 10 m above water level wind vector. Full details of the calculation of wave stress, total stress, and the enhanced drag coefficient are given in Janssen (1991).

Coupling requires the CH3D model to send arrays of surface current and water elevation to WAM; the water elevations are used to update the total water depths. The governing equation of WAM is the spectral energy conservation equation in spherical co-ordinates:

$$\frac{\partial E}{\partial t} + \frac{\partial (\dot{l} E)}{\partial l} + \frac{\partial (\dot{f} E)}{\partial f} + \frac{\partial (\dot{s} E)}{\partial s} + \frac{\partial (\dot{q} E)}{\partial q} = S_{in} + S_{nl} + S_{bf} + S_{wc}, \tag{6}$$

where $E = E(s, q, l, f, t)$; q is wave direction; l is longitude; f is latitude; the dotted terms are partial derivatives with respect to time; $S_{in} = S_{in}(s, q, l, f, t)$ is the wind input source term; S_{nl} is the wave-wave nonlinear interaction source term; S_{bf} is the bottom friction sink term; and S_{wc} is the whitecapping sink term. This equation is written in terms of the relative frequency, s, for a frame of reference moving with the current. The relation between s and the frequency for a fixed frame of reference is

$$w = s + \tilde{k} \cdot \tilde{U}, \tag{7}$$

where $\tilde{k}$ is the wavenumber vector and $\tilde{U}$ the current vector. The partial derivative terms in (6) contain several occurrences of the current vector and water depth (Zhang et al., 1998). These coupling effects represent current-induced wave refraction and propagation, and depth-induced wave refraction. In the basic version of WAM cycle-4, the source/sink terms in (6) are calculated using the algorithms from earlier versions of the code (WAMDI, 1988) which did not account for the presence of currents. This ignores the fact that the effective wind vector and the motion of waves relative to bed roughness elements are altered by the adoption of the moving frame of reference. These changes have no effect on the S_{nl} and S_{wc} algorithms, but the S_{in} and S_{bf} calculations must be modified. In this research, S_{in} is calculated using the effective wind vector

$$\tilde{u}'_{10} = \tilde{u}_{10} - \tilde{U}, \tag{8}$$

and S_{bf} is calculated using w, calculated from (7), rather than s.

Lake Michigan Hindcasts

Lake Michigan hindcasts have been performed for Julian days 86 through 89 (March 27th through April 9th), 1998. This period was selected based on event magnitude and data availability. During the period, buoy data included winds up to 13 m/s and significant wave heights up to 3 m. Conditions were quiescent on day 86, which provided an opportunity for realistic model spin-up. Meteorological observations from the National Weather Service were used in the interpolation of hourly grids of air temperature, dew point, cloud cover, and wind components. The wind observations were adjusted to 10 m above water level and also corrected for the effect of overland to oversea roughness differences (Schwab and Morton, 1984). The interpolated wind fields were used as inputs to both models and the other interpolated fields were used to calculate the surface heat flux inputs also required by CH3D (Cotton, 1979; Edinger et al., 1974). Hindcasts were run for no model coupling, one-way coupling (each model reads the other model's no-coupling results from file once per hour), and two-way coupling using coupling time-steps of 60 minutes and 3 minutes.

Figure 1 shows contours and vectors of WAM significant wave heights at hour-216 of the no-coupling hindcast. The axis scales refer to the 67 x 139 computational grid. At hour-216 the winds were predominantly from the north, with a typical magnitude of 10 m/s. This resulted in fetch-limited wave growth over most of the lake, with the maximum wave height occurring close to the southern shore, at cell (15,10). Figure 2 shows CH3D surface current vectors and water elevation contours at hour-216 of the no-coupling hindcast. It can be seen that the northerly wind causes a storm surge and associated maximum surface currents in the south of the lake. Figures 3 and 4 show the CH3D predictions at hour-216 of the two-way coupled hindcasts with coupling time steps of 60 minutes and 3 minutes, respectively. Comparing these figures with figure 2 shows that the interactions with the waves have significantly increased the CH3D storm surge and surface currents. It is also evident that the coarser coupling time-step results in the greatest surge and currents. The reason for this is that the infrequent feedback between the two models' wave-current interactions in the 60-minute coupling run results in an overshoot of the coupling effects. Figures 5 and 6 show the WAM predictions at hour-216 for the 60-minute and 3-minute coupling time-steps, respectively. Comparing these figures with figure 1, one can see that the current effects in WAM have slightly reduced the wave heights, due to reduced effective wind velocities. There is also further evidence that the coarser coupling time-step results in an overprediction of the coupling effects. Results are not shown for the one-way coupling hindcast, but in that case the overprediction of the coupling effects was larger than in the coarse two-way coupling hindcast. This is to be expected since there is no feedback between the two models' coupling effects.

In general the Lake Michigan hindcasts indicated that coupling increases CH3D storm surges and surface currents on the order of 20 %. In continental shelf waters this would translate to increased surges on the order of several feet, which could greatly influence the planning of military operations. The coupling effects in WAM typically modified wave heights on the order of 3 %, but impact would be greater in high current regions

such as the Gulf Stream. One-way coupling overpredicted coupling effects on the order of 25 % and two-way coupling only every 60 minutes overpredicted effects on the order of 10 %.

The hindcast predictions of water elevation and wave height were compared with data. The coupling effects noticeably affected how predicted time series matched with observations, but there was no conclusive proof that the coupled hindcast predictions were more accurate. The reasons for this were the low “signal to noise” ratios. The coupling effects on waves were small, and while the coupling effects on storm surges were significant, the surges themselves were relatively small. Furthermore, the circulation patterns in some of the interpolated wind fields used to drive the hindcasts were clearly unrealistic. Future hindcasts should model a location where storm surges are on the order of meters and should use wind fields from meteorological simulations. Future hindcasts will also target locations of military significance.

Scalability and the Effect of Grid Size

The scalability of the coupled CH3D/WAM system and the individual parallel codes has been measured. Wallclock timings were recorded for 24-hour simulations using the 4-km (67 x 139) Lake Michigan grid described above and also a 2-km (133 x 252) Lake Michigan grid. It was found that the time required for a stand-alone OpenMP WAM run was equal to the time required for a coupled run involving the same number of WAM threads. Furthermore, the number of CH3D processes used in a coupled run was found to have no effect on the time required. The explanation for these results is that the WAM model is far more computationally demanding than the CH3D model.

Figures 7 and 8 show the scalability of the coupled system on the O2K platform for the 4-km and 2-km grids, respectively. One CH3D process was used in each run. It can be seen that the reduction in execution time extends to a higher number of WAM threads for the finer grid, as one would expect. Both timing curves level off at a relatively low number of threads, however. As stated above, efficient OpenMP directives have so far been established for only the four most demanding WAM subroutines. The PFA automatic parallel directives used in the remainder of the code may have a minor, or possibly negative, effect on the scalability of the code.

The scalability of the parallel CH3D model is shown in figures 9 and 10 for the 4-km and 2-km grids, respectively. These results are for the Cray T3E platform, but the shapes of the O2K timing curves are very similar. One can see that scalability extends much farther for CH3D than for WAM, with the curves leveling off around 32 and 64 processors, respectively. In this case the size of the grids is the dominant cause of the limits. The 4-km grid has 3932 water cells. This means that for 32 processors, the domain decomposition strategy in CH3D results in each processor performing calculations for typically 4 rows and 120 cells. For such small blocks, the MPI communication overhead becomes significant and offsets the benefit of further increasing the number of processors.

Conclusions

This research entailed the coupling of sophisticated marine circulation and wind-wave models at the atmospheric boundary layer. The MPI-based parallel CH3D code and the OpenMP-based parallel WAM code were coupled, with MPI calls used for inter-model communication. The use of OpenMP restricts WAM to shared memory multi-processing architectures until OpenMP is ported to other parallel architectures. Cross-platform coupling is possible, however, through use of the MPI_Connect library.

Lake Michigan hindcasts were performed to evaluate the importance and accuracy of the model coupling. In the hindcasts, coupling effects increased storm surges and surface currents on the order of 20 %, and reduced wave heights on the order of 3 %. It was also found that frequent passing of arrays between the models was required. For a coarse coupling time-step of 60 minutes, coupling effects were overpredicted on the order of 10 % in comparison with coupling every 3 minutes. If one-way coupling was used, the overprediction rose to 25 %. Comparisons were made between predicted and observed water elevations, but the results were inconclusive due to the relatively small Lake Michigan storm surges and the large errors in the interpolated wind fields used to drive the hindcasts. It was concluded that future evaluations should use wind fields from meteorological models and a test location where surges are larger. It would also be beneficial to select a location of strategic importance to the military.

The scalability of the coupled system and component models was measured using 4-km and 2-km Lake Michigan grids. WAM is far more computationally demanding than CH3D and the time required for a coupled run was found to equal to the time required for a stand-alone WAM run with the same number of threads. Speed-up of the coupled simulations leveled off at 8 and 16 WAM threads for the 4-km and 2-km grids, respectively. A contributory factor to the premature leveling off is that optimized implementation of OpenMP has so far been completed in only the four most demanding WAM subroutines, totaling 50 % of sequential model execution time. The automatic PFA parallel directives used in the remaining subroutines appear to have a minor impact on performance. Stand-alone runs of the parallel CH3D code reached minimum execution times at 32 and 64 processors for the 4-km and 2-km grids, respectively, with these limits due to grid sizes.

In conclusion, the use of high performance computing facilities permits these important marine forecasts to be generated more quickly and/or at a higher resolution. The parallel CH3D/WAM system will at present generate marine forecasts up to three times faster than the sequential system. If the scalability of WAM could be increased to that of CH3D, this ratio would rise to approximately ten. Further efforts to improve WAM scalability are justifiable due to the potential impact on military operations.

Acknowledgement

This work was supported in part by the DoD HPC Modernization Program.

References

Bangalore, P. V., Zhu, J., Huddleston, D., Skjellum, A., Welsh, D. J. S., Bedford, K. W., Wang, R. and Sadayappan, P. (1999). Parallelization of a coupled hydraulics and sediment transport model, *CEWES MSRC PET Technical Report*, Mississippi State University and The Ohio State University. Prepared for the Department of Defense HPC Modernization Program.

Bova, S. W., Breshears, C. P., Cuicchi, C., Demirbilek, Z. and Gabb, H. A. (1999). Dual-level parallel analysis of harbor wave response using MPI and OpenMP, submitted to *International Journal of High Performance Computing Applications*.

Chapman, R. S., Johnson, B. H. and Vemulakonda, S. R. (1996). User's guide for the sigma stretched version of CH3D-WES; a three-dimensional numerical hydrodynamic and temperature model, *Technical Report HL-96-21*, U.S. Army Engineer Waterways Experiment Station, Vicksburg, MS.

Cotton, G. F. (1979). ARL models of global solar radiation, in *Hourly Solar Radiation – Surface Meteorological Observations. Solmet, Volume 2, Final Report*, National Climate Center, Department of Energy.

Edinger, J. E., Brady, D. K. and Geyer, J. C. (1974). Heat exchange and transport in the environent, *Electric Power Research Institute publication no. 74-049-00-3*, EPRI, Palo Alto, CA.

Glenn, S. M. and Grant, W. D. (1987). A suspended sediment stratification correction for combined wave and current flows, *Journal of Geophysical Research* **92**: 8244—8264.

Gunther, H., Hasselmann, S. and Janssen, P. A. E. M. (1992). The WAM model cycle 4, *Technical Report*, Deutsches KlimaRechenZentrum, Hamburg, Germany.

Holthuijsen, L. H. and Tolman, H.L. (1991). Effects of the Gulf Stream on ocean waves, *Journal of Geophysical Research* **96**: 12755-12771.

Komen, G. J., Cavalieri, L., Donelan, M., Hasselmann, K., Hasselmann, S. and Janssen, P. A. E. M. (1994). *Dynamics and Modelling of Ocean Waves*, Cambridge University Press, Cambridge, U.K.

Phillips, O. M. (1977). The sea surface, *Modelling and Prediction of the Upper Layers of the Ocean*, Pergamon Press, Elmsford, NY, pp. 229-237.

Schwab, D. J. and Morton J. A. (1984). Estimation of overlake wind speed from overland wind speed: a comparison of three methods, *Journal of Great Lakes Research* **10**: 68-72.

WAMDI (1988). The WAM model – a third generation ocean wave prediction model, *Journal of Physical Oceanography* **18**: 1775-1810.

Welsh, D. J. S., Wang, R., Sadayappan, P. and Bedford, K. W. (1999). Coupling of Marine Circulation and Wind-Wave Models on Parallel Platforms, *CEWES MSRC PET Technical Report*, The Ohio State University, Columbus, OH. Prepared for the Department of Defense HPC Modernization Program.

Zhang, S., Welsh, D., Bedford, K., Sadayappan, P. and O'Neill, S. (1998). Coupling of circulation, wave and sediment models, *Technical Report CEWES MSRC/PET TR/98-15*, The Ohio State University, Columbus, OH. Prepared for the Department of Defense HPC Modernization Program.

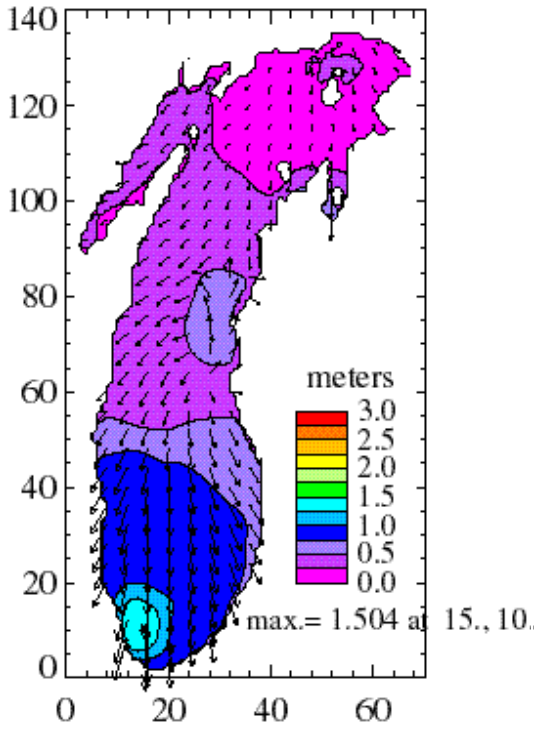

Figure 1: WAM wave heights at hour-216 of EEGLE hindcast for no coupling

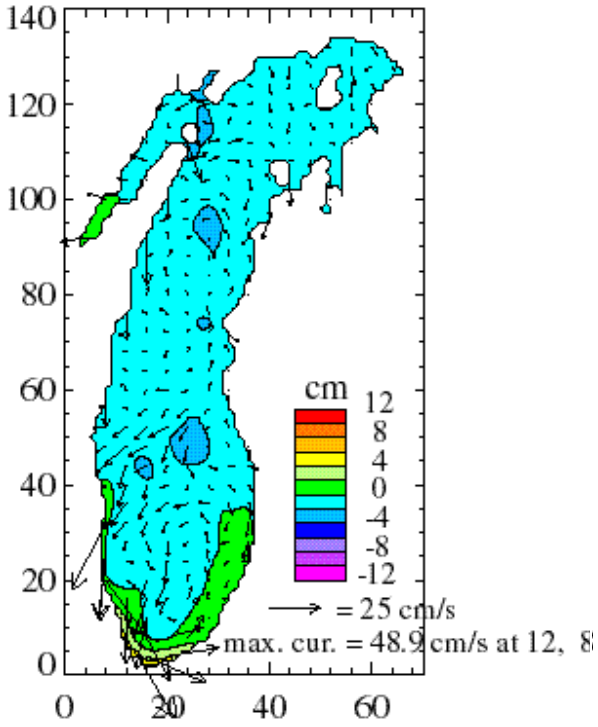

Figure 2: CH3D surface currents and elevations at hour-216 of EEGLE hindcast for no coupling

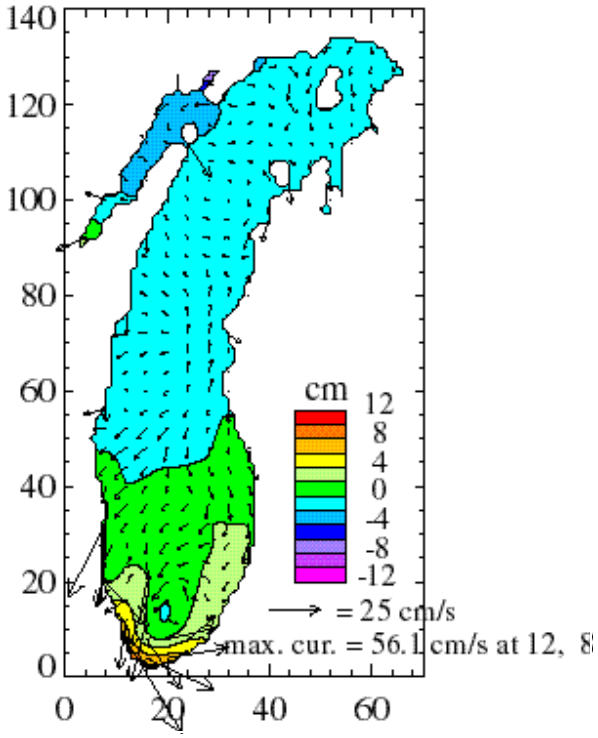

Figure 3: CH3D surface currents and elevations at hour-216 of EEGLE hindcast for two-way coupling every 60 minutes

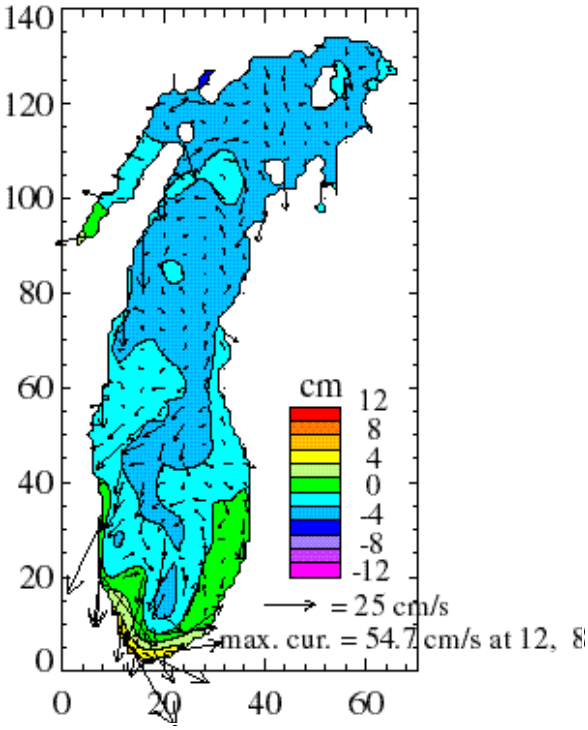

Figure 4: CH3D surface currents and elevations at hour-216 of EEGLE hindcast for two-way coupling every 3 minutes

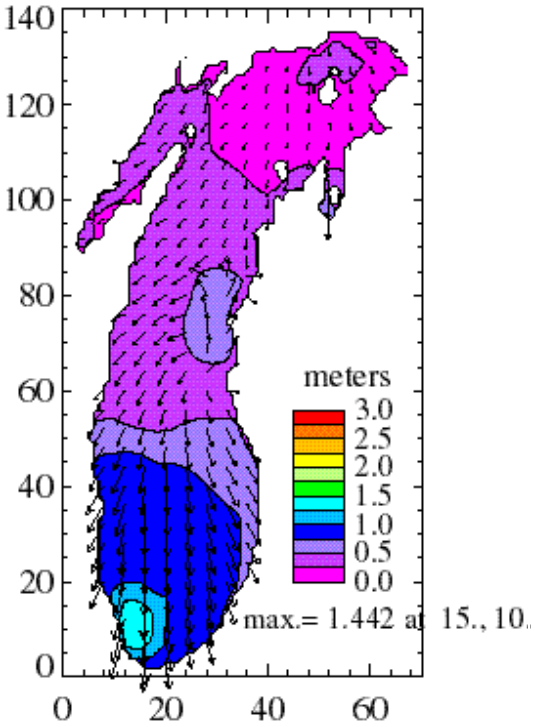

Figure 5: WAM wave heights at hour-216 of EEGLE hindcast for two-way coupling every 60 minutes

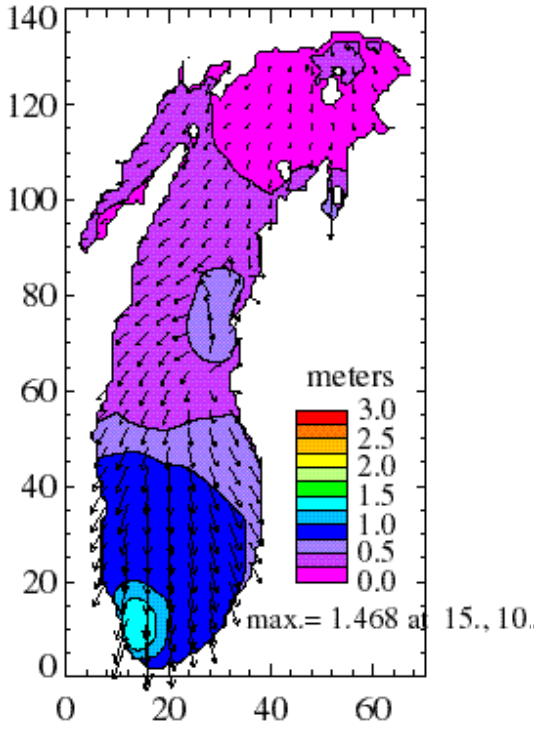

Figure 6: WAM wave heights at hour-216 of EEGLE hindcast for two-way coupling every 3 minutes

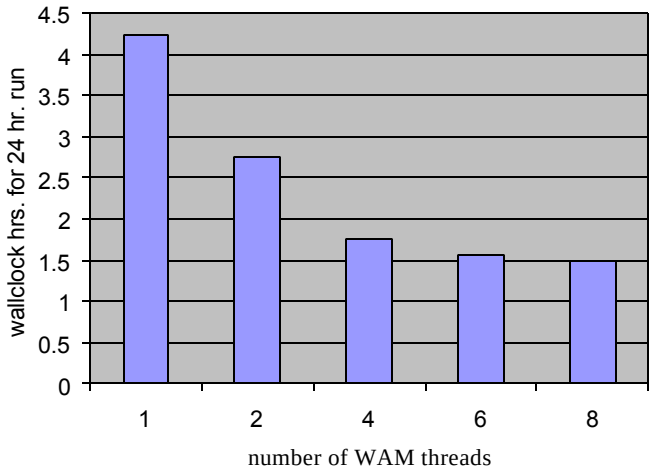

Figure 7: Scalability of coupled CH3D/WAM on the O2K for the 4-km L. Michigan grid

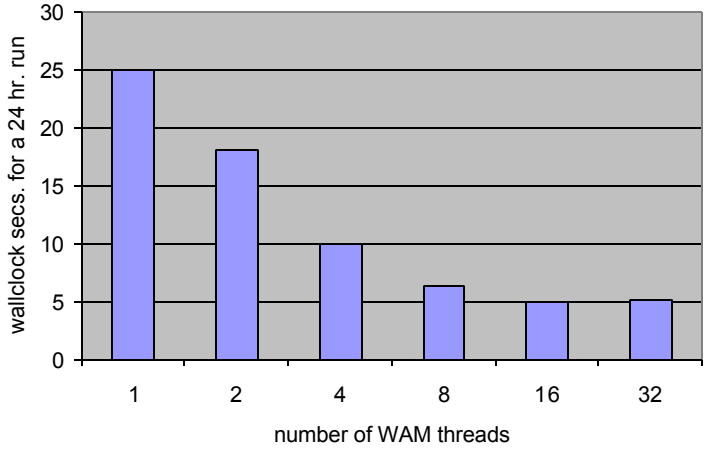

Figure 8: Scalability of coupled CH3D/WAM on the O2K for the 2-km L. Michigan grid

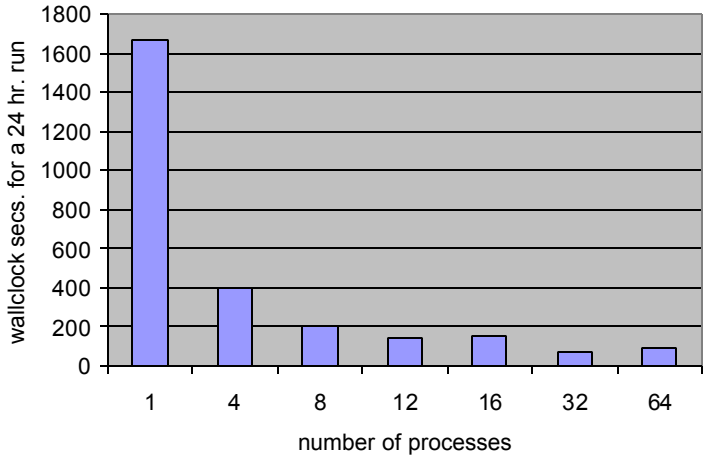

Figure 9: Scalability of parallel CH3D on the T3E for the 4-km L. Michigan grid

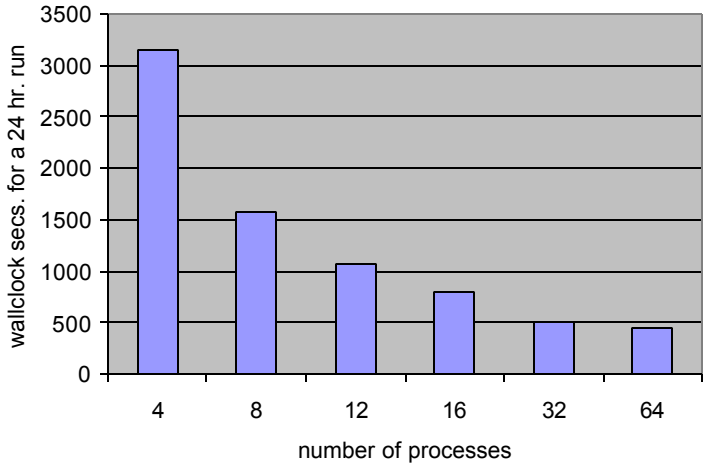

Figure 10: Scalability of parallel CH3D on the T3E for the 2-km L. Michigan grid